

# One Ring to Encompass them All: A giant stellar structure that surrounds the Galaxy

R. A. Ibata<sup>1</sup>, M. J. Irwin<sup>2</sup>, G. F. Lewis<sup>3</sup>, A. M. N. Ferguson<sup>4</sup>, N. Tanvir<sup>5</sup>

<sup>1</sup> *Observatoire de Strasbourg, 11, rue de l'Université, F-67000, Strasbourg, France*

<sup>2</sup> *Institute of Astronomy, Madingley Road, Cambridge, CB3 0HA, U.K.*

<sup>3</sup> *School of Physics, University of Sydney, NSW 2006, Australia*

<sup>4</sup> *Kapteyn Astronomical Institute, Postbus 800, 9700 AV Groningen, The Netherlands*

<sup>5</sup> *Physical Sciences, Univ. of Hertfordshire, College Lane, Hatfield, AL10 9AB, UK*

1 November 2018

## ABSTRACT

We present evidence that the curious stellar population found by the Sloan Digital Sky Survey in the Galactic anticentre direction extends to other distant fields that skirt the plane of the Milky Way. New data, taken with the INT Wide Field Camera show a similar population, narrowly aligned along the line of sight, but with a Galactocentric distance that changes from  $\sim 15$  kpc to  $\sim 20$  kpc (over  $\sim 100^\circ$  on the sky). Despite being narrowly concentrated along the line of sight, the structure is fairly extended vertically out of the plane of the Disk, with a vertical scale height of  $0.75 \pm 0.04$  kpc. This finding suggests that the outer rim of the Galaxy ends in a low-surface brightness stellar ring. Presently available data do not allow us to ascertain the origin of the structure. One possibility is that it is the wraith of a satellite galaxy devoured long ago by the Milky Way, though our favoured interpretation is that it is a perturbation of the disk, possibly the result of ancient warps. Assuming that the Ring is smooth and axisymmetric, the total stellar mass in the structure may amount to  $\sim 2 \times 10^8 M_\odot$  up to  $\sim 10^9 M_\odot$ .

**Key words:** Galaxy: structure – Galaxy: disk – galaxies: interactions

## 1 INTRODUCTION

Due to our location within the disk of the Milky Way, studies of the global structure of this galactic component are hampered by projection problems, crowding, dust, and the presence of intervening populations (such as the Bulge). Nowhere is this so problematic as in the study of the very outer edge of the disk. The advent of the recent wide-area infra-red surveys (e.g. 2MASS and DENIS) have alleviated the extinction problem, but the other problems remain, with the distance ambiguity being particularly limiting. Even the future astrometric mission GAIA (Perryman et al. 2001) is unlikely to give us a full picture of the Galactic disk, due to telemetry limits in regions of high stellar density.

Yet the outer regions of galactic disks are important regions to study, as they provide important clues to our understanding of the global structure and formation of galaxies (see, e.g., van der Kruit 2001). These are the least self-gravitating regions of galactic disks, and the presence of the dark matter halo can begin to be felt at these radii. The flaring of the outer disk constrains the dark matter fraction in these regions (Olling & Merrifield 2000, and references therein). Perhaps the most interesting aspect of the very outermost edge of the disk is that it is expected

to be young. In galaxy formation simulations that contain a gas component as well as Cold Dark Matter, galaxy disks tend to grow from the inside out, with the most recently accreted gas settling down onto the end of the disk (Navarro & Steinmetz 1997). Ensuing star-formation in regions of sufficient density produces young stars, leading to a primarily young, metal-poor stellar population in these galactic extremities, though radial mixing in the disk may smear this information out (Sellwood & Binney 2002). However, recent simulations (Sommer-Larsen, Gotz & Portinari 2002) show that some disks form outside-in as well as inside-out, in agreement with tantalising new evidence that indicates that the outer disk of the Andromeda galaxy may well be old (Ferguson & Johnson 2001). Determining the age of disk populations at large radius will provide a good test of current disk formation models.

An interesting recent development in the study of the stellar populations of the outer disk has been presented by Newberg et al. (2002), based on Sloan Digital Sky Survey photometry of fields towards the Galactic anticentre direction. Newberg et al. (2002) find an overdensity of F-colored stars close to the Galactic plane in the constellation “Monoceros”, with a narrow colour-magnitude sequence that belies

arXiv:astro-ph/0301067v2 18 Feb 2003

a stellar population  $\sim 11$  kpc from the Sun and  $\sim 18$  kpc from the Galactic centre. The narrow magnitude spread implies a distance spread of about  $\sim 2$  kpc, despite the fact that the structure is seen over a wide range above and below the Galactic plane stretching from  $b \sim -25^\circ$  to  $b \sim 20^\circ$  (i.e.  $-5.5 \text{ kpc} < z < 4.5 \text{ kpc}$ ).

The analysis of Newberg et al. (2002) suggested that this stellar population was a very nearby orbiting Galactic satellite. Here we present evidence of similar colour-magnitude features in fields taken as part of a survey of the Andromeda galaxy with the Isaac Newton Telescope (INT), and as part of a public survey observed with the same telescope entitled the INT Wide Field Survey (WFS).

## 2 THE ISAAC NEWTON TELESCOPE WIDE FIELD CAMERA SURVEYS

The INT WFS is an initiative by the UK and Dutch communities to devote a large fraction of the INT to deep and wide-field surveys. Many fields have now been observed since 1998. However, the resulting coverage at the present time is patchy, with most time having been spent in large extragalactic surveys towards the Galactic polar caps. Table 1 is a listing of suitable WFS or WFC observations below  $|b| \lesssim 50^\circ$ . In Figure 1 we display an example of one of these fields, the Elais field N1, located at  $\ell = 85^\circ$ ,  $b = +44^\circ$ , which shows the normal Galactic stellar population sequences. In contrast, Newberg et al. (2002) have shown that the anti-centre (“Monoceros”) region shows an additional feature in colour-magnitude space (their Figure 12), with shape similar to a main sequence that has a turnoff at  $g' - r' = 0.25$ ,  $g' \sim 19.5$  (in the AB system).

In examining INT WFC survey fields, we have detected the presence of this unexpected feature in other distant fields. Figure 2 displays the colour-magnitude diagram of the INT WFC field “Mono-N” (located at  $\ell = 150^\circ$ ,  $b = +20^\circ$ ); a population that follows a track similar to a narrow-main sequence is seen in addition to the usual Galactic components. This sequence is shown more clearly in the right-hand panel of Figure 3, in which we have used the Elais-N1 field as a “background” to subtract off the normal Galactic components. Due to the difference in Galactic latitude between the target and control fields, the thick disk is not subtracted cleanly: this poor subtraction of the thick disk is seen as a smear to brighter magnitudes and redder colours than the narrow sequence that delineates the abrupt faint end of the right hand panel of Figure 3. Another INT WFS field that displays this excess population is the field named WFS-0801 ( $\ell = 180^\circ$ ,  $b = +30^\circ$ ), the colour-magnitude diagram of which is displayed in Figure 4. Subtracting a background estimated from the Elias-N1 field gives the Hess diagram displayed on the right-hand panel of Figure 5. As the “background” field is closer in Galactic latitude to the WFS-0801 field, this statistical subtraction is much cleaner, allowing us to show the unexpected excess population relatively free of contamination from the expected Galactic components.

The other two proprietary large surveys (Ibata et al. 2001; Ferguson et al. 2002, 2003) were conducted by our group to reveal the structure and stellar populations in the halo of the Andromeda galaxy ( $\ell = 122^\circ$ ,  $b = -21^\circ$ ) and M33 ( $\ell = 134^\circ$ ,  $b = -31^\circ$ ). A further two fields were ob-

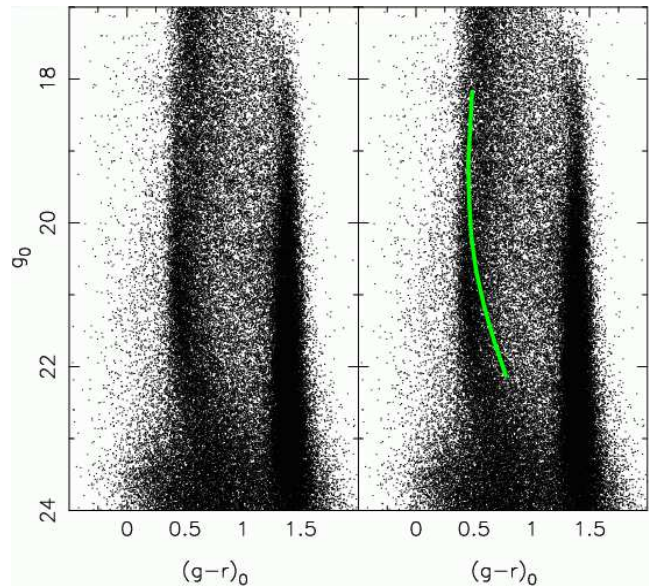


**Figure 1.** The colour-magnitude diagram of the Elais field N1 ( $\ell = 85^\circ$ ,  $b = +44^\circ$ ), which we will use as a control field. This comparison region shows the usual Galactic components. The Galactic disk dwarfs contribute to the well-populated red vertical structure at  $(g-r)_0 \sim 1.4$ , whereas the progressive main-sequence turnoffs of the thick disk and halo give rise to the blue vertical structure at  $(g-r)_0 \sim 0.5$ . Eventually, at magnitudes fainter than  $g_0 \sim 22$  the halo sequence curves round to the red due to the rapidly-falling density at large Galactocentric distance. (The photometry has been corrected for extinction using the maps of Schlegel et al. 1998). The right-hand panel shows the same data as the left-hand panel, but we have superposed the ridge-line of the structure of interest in Figures 2–5 to serve as a visual aid in the interpretation of those figures. Note that the narrow stellar sequence detected in fields Mono-N1 (Figures 2 and 3) and in WFS-0801 (Figures 4 and 5), which lies close to the ridge line, is not present in this comparison field.

served for use as comparison regions for these surveys. Table 1 also lists these fields. In Figures 6 and 8 we display the  $V_0$ ,  $(V-i)_0$ , colour-magnitude diagram in our M31 survey, where we have plotted separately the northern (lower  $|b|$ ) and southern quadrants of the survey. The CMD structure seen in the SDSS “Monoceros” field is also observed in our 30 square-degree field around M31. The left-hand panel of Figure 7 shows the Hess diagram of the northern M31 field (note that this is a zoomed-in view of Figure 6). Lacking an appropriate background field in  $V$  and  $i$  pass-bands, we have been forced to use the southern M31 field as a comparison region. The result of subtracting the southern M31 field from the northern M31 field is displayed in the right-hand panel of Figure 7; the excess population is again clearly seen as a narrow sequence.

The high statistical significance of the detection of the excess population in the different fields is demonstrated in Figure 9, where we show the distribution of stars as a function of their displacement in colour from the ridge-lines. Due to the lack of a suitable background field, we are unable to provide a similar estimate of the significance of the detection in the southern M31 field, though the population is clearly present in that field, as we show in Figure 10.

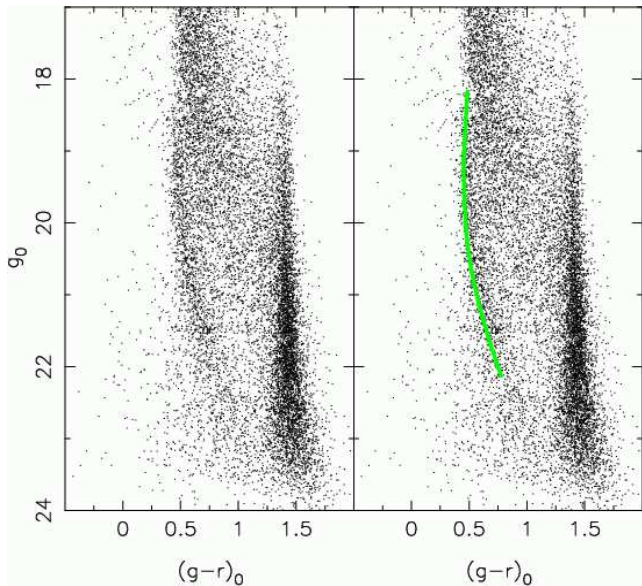


**Figure 2.** The colour-magnitude diagram of a field (Mono-N) at  $\ell = 150^\circ$ ,  $b = +20^\circ$ . An additional colour-magnitude feature is present here over the expected disk, thick disk and halo components, and is seen as a narrow CMD structure, similar to a main sequence with turn-off at  $(g-r)_0 \sim 0.5$ ,  $g_0 \sim 19.5$  (in the Vega system). Correcting for the difference between the AB and Vega photometry, we see that the peculiar main-sequence detected by Newberg et al. (2002) in Sloan Digital Sky Survey (SDSS) data towards the Galactic anticentre is also clearly present in this field. We used the colour transformations outlined in the text to convert the ridge-line of the feature in the SDSS S223+20 field; an offset of  $-0.4$  magnitudes was needed to match up the sequences, implying that the structure in the S223+20 field is more distant. The right-hand panel shows this ridge-line overlaid on the colour-magnitude diagram. The similarity in the turn-off colour of this feature and that of the Galactic thick disk and halo shows that its stellar population is of comparable age to those ancient Galactic components.

### 3 RESULTS AND CONCLUSIONS

The detection of a stellar population almost identical to that seen in the SDSS Monoceros fields shows that this structure is immense. The M31 field is  $\sim 100^\circ$  away in longitude from the S223+20 field, towards the diametrically opposite side of the Galaxy. The structure is also seen both below the Galactic plane (in the M31 field and in S200-24) and above it (in fields Mono-N, WFS-0801, S183+22, S218+22, and S223+20), covering a vertical range of more than  $50^\circ$ . The fields at higher Galactic latitude than  $|b| \sim 30^\circ$  did not show up a similar CMD feature, and neither was the feature detected in the lower latitude ( $b = -31^\circ$ ) M33 field. The structure appears to be confined close to the Galactic plane.

To investigate the difference in Heliocentric distance between the fields, we compared the colour-magnitude sequence detected by Newberg et al. (2002) in the S223+20 field to the three INT fields Mono-N, WFS-0801, and M31. Due to the difference in the photometric systems between the surveys, conversions need to be made to shift measurements in the SDSS  $(g',r')$  system to Vega-normalized  $(g,r)$  and  $(V,i)$ . For the  $(g,r)$  fields we used an South Galactic Pole region where there are overlapping INT and SDSS data (the latter from the Early Data Release, Stoughton et al. 2002);

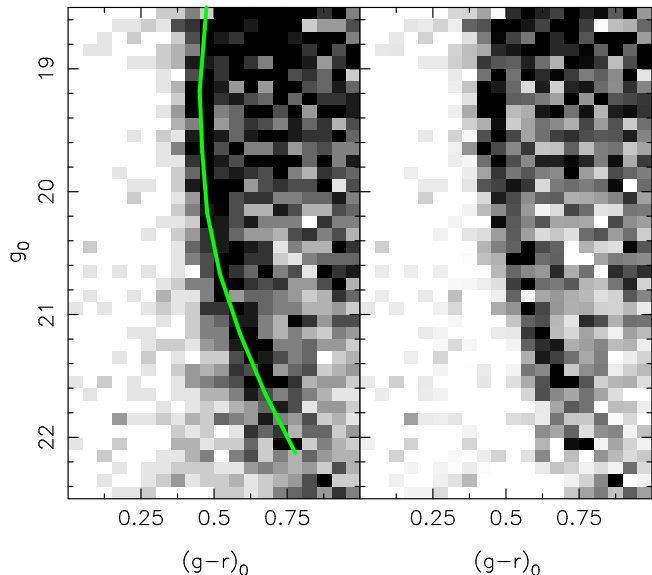


**Figure 3.** The left hand panel shows a (zoomed-in) Hess diagram of the Mono-N field previously presented in Figure 2 (the ridge-line of Figure 2 has been reproduced here as well). The right-hand panel shows the result of subtracting the Hess-diagram of the Elais-N1 comparison region from these data. The halo contribution, which lies primarily at fainter magnitudes than the ridge line, is similar in the two fields, so the subtracted Hess diagram is relatively well cleaned of halo contaminants. However, the comparison field (which is located at  $b = +44^\circ$ ) has a substantially lower surface density of thick disk stars than the Mono-N field, so the thick disk contribution is only slightly reduced in the subtracted Hess diagram. Nevertheless, the narrow colour-magnitude sequence can be clearly perceived. The colour distribution around the sequence shows a narrow peak with  $S/N > 20$  (see Figure 9).

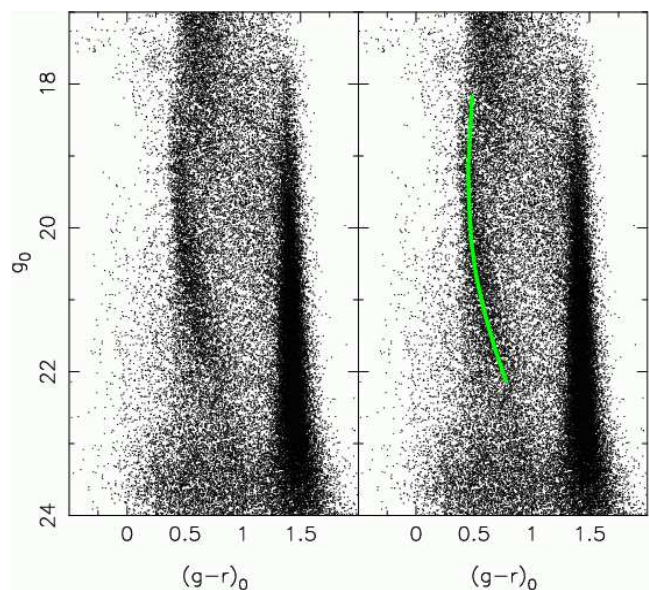


**Figure 4.** As Figure 2, but for the INT WFS-0801 field at  $\ell = 180^\circ$ ,  $b = +30^\circ$ . An offset of  $-0.4$  magnitudes is needed to match up this sequence to that of the S223+20 field.

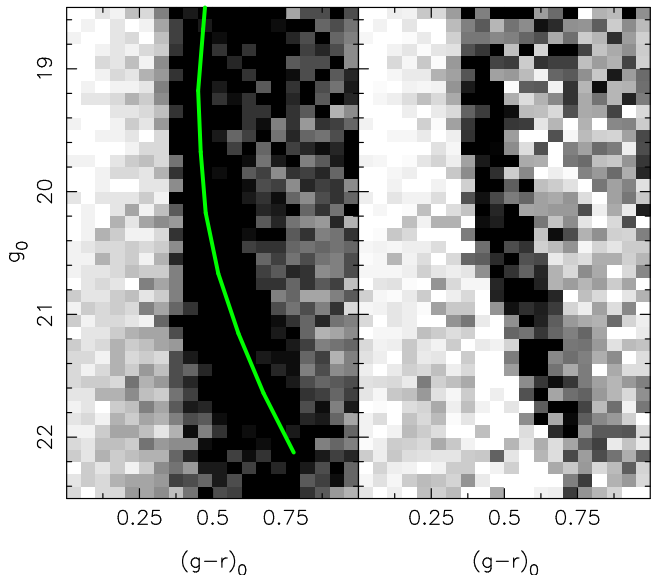


**Figure 5.** In a similar manner to Figure 3, the right-hand panel shows the Hess diagram of the INT WFS-0801 field at  $\ell = 180^\circ$ ,  $b = +30^\circ$ . The left-hand panel displays the result of subtracting the Elais-N1 comparison region from the data in the right-hand panel. Due to the smaller difference in Galactic latitude between the WFS-0801 field and the Elais-N1 field, the subtraction of the thick disk component is cleaner than in Figure 3, and the excess population stands out very clearly. Figure 9 shows that the excess is detected at  $S/N > 30$ .

we find  $(g - r) = 0.21 + 0.86(g' - r')$  and  $g = g' + 0.15 - 0.16(g - r)$ . The resulting transformed track of the S223+20 field requires an offset of  $-0.4$  mag to match the Mono-N and WFS-0801 fields (i.e. stars in the Mono-N and WFS-0801 features are brighter). To convert to  $(V, i)$  we took  $V = g - 0.03 - 0.42(g - r)$  (Windhorst et al. 1991), and used the WFS photometry in the WFS-2240 field to find the following necessary transformation:  $(g - i) = 0.09 + 1.51(g - r)$ . The offset of the S223+20 ridge-line was found to be  $-0.8$  mag for the northern M31 field (the feature in the southern M31 field has too low S/N to fit). Assuming that the S223+20 feature is 11 kpc distant (Newberg et al. 2002), and interpreting these magnitude offsets as due to distance variations, puts the structure in the Mono-N, WFS-0801 and M31 fields at a distance of  $\sim 9$  kpc,  $\sim 9$  kpc and  $\sim 8$  kpc respectively. The corresponding Galactocentric distances, in order of increasing Galactic longitude<sup>1</sup>, are:  $\sim 14$  kpc in M31 (at  $\ell = 123^\circ$ ),  $\sim 16$  kpc in Mono-N (at  $\ell = 149^\circ$ ),  $\sim 16$  kpc in WFS-0801 (at  $\ell = 180^\circ$ ), and 17.7 kpc in S223+20 (at  $\ell = 221^\circ$ ).

The substantial area of our M31 field allows a first estimation of the scale-height of this unexpected population. To this end we selected stars in a banana-shaped region between  $20.5 < V_0 < 21.5$  and  $0.5 + 0.02(V_0 - 17.0)^2 < (V - i)_0 < 0.8 + 0.02(V_0 - 17.0)^2$ . The density of these sources is displayed as filled circles

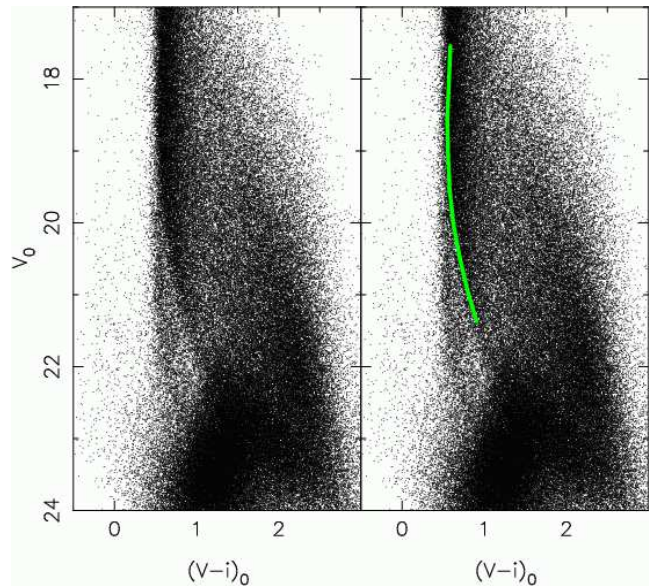


**Figure 6.** The colour-magnitude diagram of the northern M31 field ( $\ell = 123^\circ$ ,  $b = -19^\circ$ ). A numerous main-sequence shaped colour-magnitude structure is seen from  $(V - i)_0 \sim 0.5$ ,  $V_0 \sim 19$  curving red-wards to  $(V - i)_0 \sim 1.0$  at  $V_0 \sim 21.5$ . Although this diagram cannot be compared directly to Figures 2 or 4, or to the SDSS CMD of the “Monoceros” population, due to the different photometric passbands, its behaviour is strikingly similar. The additional stars with  $V_0 \gtrsim 22$  are the top two magnitudes of the red giant branch in the halo of M31. The ridge-line of the SDSS S223+20 feature, converted to  $(V, i)$ , requires a significant offset of  $\sim -0.8$  magnitudes to make the two sequences coincide. The right-hand panel shows this ridge-line.

in Figure 10, and shows a rapid rise towards the Galactic plane. After subtracting a “background” level measured from the same colour-magnitude region in the M33 field ( $b = -31^\circ$ ), we performed a straight-line fit to the logarithm (base-ten) of the counts per square degree, which yields a slope of  $0.081 \pm 0.004$  per degree of Galactic latitude. Taking the distance of 8 kpc derived above, this implies a scale height of  $0.75 \text{ kpc} \pm 0.04 \text{ kpc}$ . The open circles in Figure 10 show a similar selection, just slightly bluer, which picks out Galactic halo stars. In contrast, this second selection gives an almost flat distribution, consistent with our preconceptions of the Halo as an almost spherically-distributed component.

The nature of this structure remains a puzzle. It is clear that it cannot be related to the normal thin disk, as it lies several magnitudes below the expected thin disk sequence. The rapid decline in the density of the feature away from the Galactic plane also rules out a direct connection to the halo. This leaves the thick disk as the only normal Galactic option. We used the Galaxy starcounts model of Ibata (1994) to predict the  $B - V$ ,  $V$  colour-magnitude diagram of the thick disk in all of the fields investigated ( $B - V$  colours are close to  $g - r$ ). For the thick disk, we find that the spread in  $V$  magnitude at constant colour has a FWHM exceeding 3 magnitudes in all of our fields (we chose to sample 0.05 magnitudes about  $B - V = 1.0$  which gives the minimum spread in magnitude). The detected feature therefore cannot be the standard thin disk, halo or even thick disk, in

<sup>1</sup> Please note that the photometric conversions, especially the extrapolation from  $(g', r')$  on the AB system to  $(V, i)$  on the Vega system, may have significant systematic errors. The estimated distances are therefore only indicative.

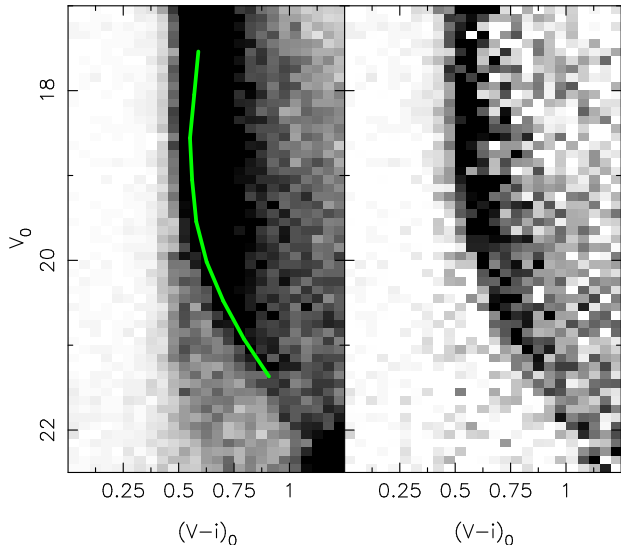


**Figure 7.** The left-hand panel shows the Hess diagram of the northern M31 field ( $\ell = 123^\circ$ ,  $b = -19^\circ$ ). This is a zoomed-in view of Figure 6; the ridge-line of Figure 6 is also reproduced here to guide the eye. The right-hand panel is the result of subtracting the southern M31 field ( $\ell = 122^\circ$ ,  $b = -24^\circ$ ) from these data. Given that these two fields are so close on the sky, the halo and thick disk populations are similar, so the contamination of the halo and thick disk in the Hess diagram on the right-hand panel has been substantially reduced by the subtraction. The narrow colour-magnitude sequence stands out with  $S/N > 30$  (see Figure 9). Note, however, that the southern M31 field is not a good “background” region, since the excess population is also detected in that field (as seen in Figures 8 and 10), though in lower numbers. This means that the excess population is over-subtracted on the right-hand panel, leading to an underestimate of its significance.

agreement with Newberg et al. (2002). Several possibilities present themselves:

- i. One option is that the various surveys probe small areas of a gigantic ring that encompasses the disk. The ring has a radius of 15–20 kpc, a radial thickness of  $\sim 2$  kpc, and a vertical scale height of  $\sim 0.75$  kpc. Due to the presence of the Magellanic Clouds and the Sagittarius dwarf galaxy, the ring is warped and non-circular, explaining the variation in Galactocentric radius between some of the survey fields. The stellar mass of the structure can be estimated by taking the surface density in the M31 field as representative of the whole ring, and assuming axisymmetry and some vertical profile. If the vertical profile is exponential, as is suggested by the data displayed in Figure 10, we find that the total stellar mass of the structure is  $M = 10^9 M_\odot$ , whereas if the surface density remains constant below  $|b| = 18^\circ$ , the mass is  $M = 2 \times 10^8 M_\odot$  (for these estimates we have taken the luminosity function of Jahreis & Wielen 1997 and the mass-luminosity relation of Henry & McCarthy 1993). A possible mechanism to form such a ring may be repeated warpings of the outer disk. In the Andromeda Galaxy (seen almost edge-on), the outer stellar disk has a complicated non-axisymmetric shape (Ferguson et al. 2002), with large vertical deviations suggestive of ancient warps which now no longer follow the warp seen in the gas. The possible Ring seen in the outer disk of the Milky Way may be of similar

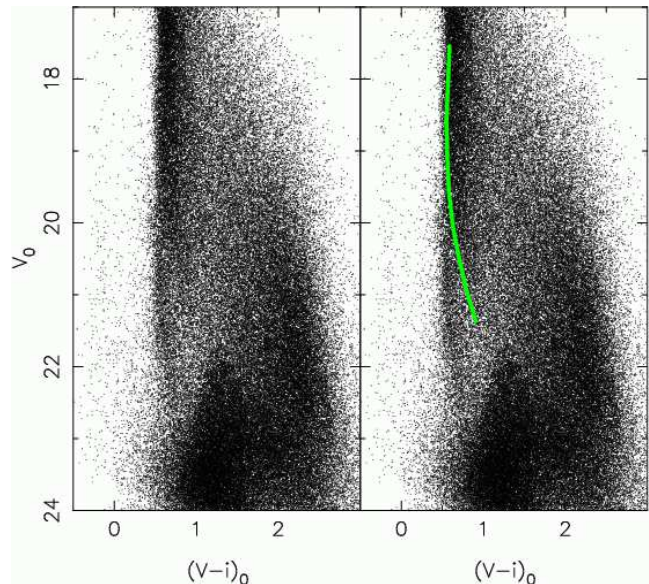


**Figure 8.** As Figure 6, but for the southern M31 field that lies further from the Galactic plane ( $\ell = 122^\circ$ ,  $b = -24^\circ$ ). The “Monoceros”-like population is still present, though much less numerous than in the northern field (which is displayed in Figure 6). To guide the eye, the location of the ridge-line in Figure 6 is shown on the right-hand panel.

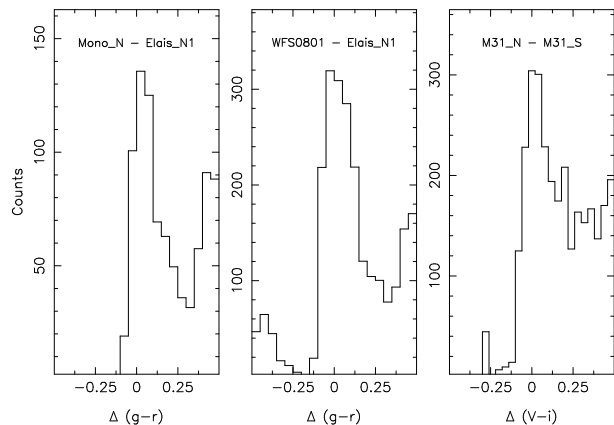


**Figure 9.** The three panels display the distribution of counts in the subtracted Hess diagrams shown in the right-hand panels of Figures 3, 5 and 7. Stars were selected in the magnitude ranges  $20.5 < g_0 < 22.0$  (for the left-hand and middle panels) and  $20.5 < V_0 < 22.0$  (for the right-hand panel), which are ranges in which the excess population in the subtracted Hess-diagrams is relatively uncontaminated. The abscissa displays the difference between the colour of the stars and the colour of the ridge-line. These narrow peaks, centered at a colour difference close to zero, show that the excess stellar population closely follows the ridge line. Fitting these narrow peaks with a Gaussian function (between  $-0.25 < \Delta \text{Colour} < 0.25$ ), gives a colour dispersion smaller than  $\sigma = 0.12$  magnitudes for all three cases. Summing under these peaks, we find that the excess population is detected with  $S/N > 20$  in the Mono-N field and with  $S/N > 30$  in the fields WFS-0801 and M31-N.

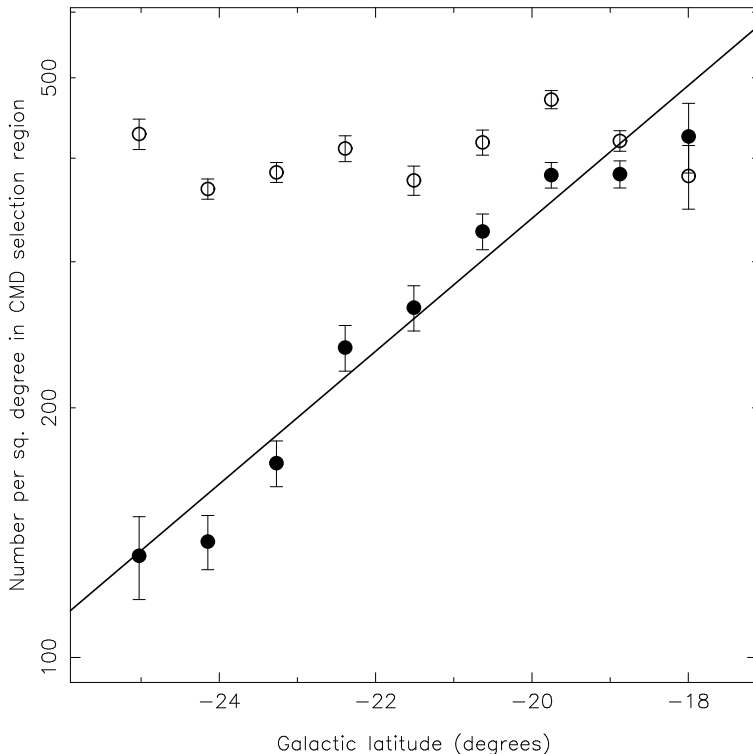


**Figure 10.** The filled circles show the density of sources (plotted on a logarithmic scale) as a function of Galactic latitude  $b$  in the M31 field that belong to the “Monoceros-like” main sequence feature that is shown in Figures 6 and 8. These sources have been selected between  $20.5 < V_0 < 21.5$ , and with colours lying between  $0.5 + 0.02(V_0 - 17.0)^2 < (V - i)_0 < 0.8 + 0.02(V_0 - 17.0)^2$ . The “background” ( $133.0 \pm 5.3$  counts per square degree, estimated from the M33 field) has been subtracted from the counts of this “Monoceros-like” population. A straight-line fit through these data is shown. The open circles show the corresponding density of normal Halo sources, selected with  $21.0 < V_0 < 22.0$ , and with colours lying between  $0.5 < (V - i)_0 < 0.4 + 0.02(V_0 - 17.0)^2$ . (No background has been subtracted from this “Halo” population).

origin. One would expect such structures to eventually mix entirely, leaving a flared outer disk, rather than a radially thin ring. Either there is another factor at play, such as, for instance, a strong interaction with the Sagittarius dwarf galaxy (Ibata & Razoumov 1998) or the Magellanic Clouds (e.g., Tsuchiya 2002), or the ring is a recent phenomenon (note however, that the stellar constituents could be older than the structure). If the structure is a perturbation, the wave may have been amplified to the current large vertical extent (in the manner of a whip) in passing outwards through the disk to regions of progressively lower density.

The low-latitude HVC field (Lewis et al. 2002), located at ( $\ell = 327^\circ$ ,  $b = -15^\circ$ ), is not in contradiction with the interpretation of the structure as a Galactic ring. Assuming that the ring has a radius of 18 kpc, implies a distance of 24 kpc in this direction, more than twice the distance to the fields in which the “Monoceros”-like CMD structure has been detected. The HVC field may simply lie too far below the Galactic plane (in that direction) to detect the Ring (the field also covers a relatively small solid angle of sky).

The reason the Ring may not have been discovered before is due to its low surface density. Very large areas need to be surveyed to detect it. It would also be difficult to detect with, for instance, the poorer photometry available from photographic plates.

ii. Another possibility is that the surveys probe different regions of the disrupted tidal stream of an accreted satellite galaxy. Halo satellites are expected to have high eccentricity orbits, with apocentre to pericentre ratio of  $\sim 4$  (van den Bosch et al. 1999). For sufficiently massive satellites ( $\gtrsim 10^9 M_\odot$ ), the continual braking effect of dynamical friction with the Galactic halo and disk can eventually lead to the decay of the orbit. However, simulations show that satellite orbits are not readily circularized by dynamical friction (van den Bosch et al. 1999; Colpi, Mayer & Governato 1999), so it is hard to explain the near circular orbit required by this scenario. A second problem relates to the small distance spread along the line of sight. As the orbit of the satellite decays, constituent stars will be lost by tidal disruption. Over time, the tidally removed stars become phased-mixed, spreading out over the orbit, and occupying the region between the orbit pericentre and apocentre. The fact that the “Monoceros”-like population is seen confined in a narrow distance interval along the line of sight therefore also argues against this scenario. The problem may be alleviated if the progenitor satellite disrupted only recently. A further concern with this scenario comes from the disruptive effect of the satellite on the Milky Way. Current cosmological simulations suggest that galaxy satellites have their own massive dark matter mini-haloes (Stoehr et al. 2002), a possibility that is supported by the high mass to light ratios inferred from small Galactic dwarf spheroidals (Mateo 1998), and from the survival requirement of the Sgr dwarf galaxy (Ibata et al. 1997; Ibata & Lewis 1998). Including the dark matter halo of a satellite that has a stellar mass in the range  $2 \times 10^8 M_\odot$  to  $10^9 M_\odot$  increases significantly the potential damage to the disk of the Milky Way, and raises the question of whether the thin disk would survive such an encounter (see, e.g., Tóth & Ostriker 1992; Velazquez & White 1999).

iii. Another possibility is that we are seeing part of an outer spiral arm, or various arm fragments. Davies (1972) has identified a variety of spiral features in the outer Galaxy via 21cm emission, extending out to a radius of  $\sim 25$  kpc. Many of these structures lie in directions where we have also detected an anomalous stellar component, leading one to speculate if these could be associated stellar arms. Indeed, if an underlying global mode were responsible for driving the spiral structure, it would not be unexpected to find an older stellar population tracing out the same pattern as the gas (e.g. Rix & Rieke 1993; Thornley & Mundy 1997). The narrow line-of-sight thickness of the structures stands in favour of this hypothesis. The thickness of the stellar component may be problematic for the spiral arm hypothesis however, although one might be able to appeal to warping to bring the bulk of the stars out of the plane.

iv. The beating motion of an asymmetric Galactic component (such as the bar) induces resonances in the disk component. However, these resonances occur very close to the plane of the disk, and stars with significant vertical motions are unlikely to partake in a strong resonance. It seems implausible, therefore, that a resonance is the cause of the detected structure.

The photometric information presented here is not sufficient to discriminate between the first three scenarios. Further photometry, especially at low Galactic latitude will be invaluable if we are to be able to properly follow the structure, and ascertain whether it is a Galactic Ring, an inhomogeneous mess due to ancient warps and disturbances, or part of a disrupted satellite stream. If this manifestly old population turns out to be the outer stellar disk, it will pose a very interesting challenge to galaxy formation models that predict inside-out assembly. Alternatively, if it transpires that the structure is due to a disrupted satellite whose orbit has been circularised and accreted along with its cargo of dark matter onto the Disk, it will provide a unique first-hand opportunity to understand the effect of massive accretions on to the inner regions of galaxies.

## REFERENCES

- van den Bosch, F., Lewis, G., Lake, G., Stadel, J. 1999, ApJ 515, 50
- Colpi, M., Mayer, L., Governato, F. 1999, ApJ 525, 720
- Davies, R. 1972, MNRAS 160, 381
- Ferguson, A., Johnson, R. 2001, ApJ 559L, 13
- Ferguson, A., Irwin, M., Ibata, R., Lewis, G., Tanvir, N. 2002, AJ 124, 1452
- Ferguson, A., Irwin, M., Ibata, R., Lewis, G., Tanvir, N. 2003, in preparation
- Henry, T., McCarthy, D., 1993, AJ 106, 773
- Ibata, R. 1994, PhD Cambridge
- Ibata, R., Wyse, R., Gilmore, G., Irwin, M. & Suntzeff, N. 1997, AJ 113, 634
- Ibata, R., Lewis, G. 1998, ApJ 500, 575
- Ibata, R. & Razoumov, A. 1998, A&A 336, 130
- Ibata, R., Irwin, M., Lewis, G., Ferguson, A., Tanvir, N. 2001, Nature 412, 49
- Jahreis, H. & Wielen, R. 1997, in: B. Battrock, M.A.C. Perryman and P.L. Bernacca (eds.): HIPPARCOS '97. Presentation of the Hipparcos and Tycho catalogues and first astrophysical results of the Hipparcos space astrometry mission, Venice, Italy, 13-16 May(1997); ESA SP-402, Noordwijk, p.675-680
- van der Kruit, P. C. 2001, ASP Conf. Ser. 230: Galaxy Disks and Disk Galaxies, 119
- Lewis, G., Irwin, M., Ibata, R., Gibson, B. 2002, PASA 19, 257
- Mateo, M. 1998, ARA&A, 36, 435
- Navarro, J., Steinmetz, M. 1997, ApJ 478, 1328
- Newberg, H., et al. 2002, ApJ
- Olling, R., Merrifield, M. 2000, MNRAS 311, 361
- Perryman, M., de Boer, K., Gilmore, G., Høg, E., Lattanzi, M., Lindegren, L., Luri, X., Mignard, F., Pace, O., de Zeeuw, P. 2001, A&A 369, 339
- Rix, H.-W., Rieke, M. J. 1993, ApJ 418, 123
- Sellwood, J., Binney, J. 2002, MNRAS 336, 785
- Schlegel, D., Finkbeiner, D., Davis, M. 1998, ApJ 500, 525
- Sommer-Larsen, J., Gotz, M., Portinari, L. 2002, astro-ph/0204366
- Stoehr, F., White, S., Tormen, G., Springel, V. 2002, MNRAS 335, L84
- Stoughton, C. et al. 2002, AJ 123, 485
- Tóth, G., Ostriker, J. 1992, ApJ 389, 5
- Thornley, M. D., Mundy, L. G. 1997, ApJ 490, 682
- Tsuchiya, T. 2002, New A. 7, 293
- Velazquez, H., White, S. 1999, MNRAS 304, 254
- Windhorst, R., Burstein, D., Mathis, D., Neuschaefer, L., Bertola, F., Buson, L., Koo, D., Matthews, K., Barthel, P., Chambers, K. 1991, ApJ 380, 362

**Table 1.** Summary of appropriate WFC observations, ordered in descending  $|b|$ . The final column lists whether the excess “Monoceros” population is detected in the field. The significance of the detection is listed for those fields where it has been possible to calculate this parameter. (The significance cannot be calculated for all of the INT fields due to a lack of suitable background fields, or of a sufficiently accurate Galaxy model). We refrain from listing the stellar density in these fields, as the values cannot be compared in a simple manner, due to the different photometric systems used in the various surveys (Figure 10 provides our current best estimate of the vertical structure of the population).

Field	RA (J2000)	Dec (J2000)	$\ell$	b	Area (sq. deg.)	Bands	Detection?
Equatorial survey	22 to 3	0:00	60 to 180	-40 to -60	$\sim 20$	g,r	NO
WFS-2240	22:40	+0:00	69	-48	9.0	g,r	NO
Elais-N1	16:13	+55:16	85	+44	9.0	g,r	NO
Elais-N2	16:36	+41:01	64	+41	9.0	g,r	NO
M33	1:34	+30:40	134	-31	4.8	V,i	NO
WFS-0801	08:02	+40:19	180	+30	7.0	g,r	$S/N > 30$
M31 comparison 2	23:50	+35	109	-26	1.2	V,i	NO
S200-24 <sup>a</sup>	5:00	+0:00	199	-25	$\sim 5$	g',r'	YES
M31-S	0:43	+38:45	122	-24	8.25	V,i	YES
S183+22 <sup>a</sup>	7:22	+35	183	+22	$\sim 5$	g',r'	YES
S218+22 <sup>a</sup>	8:16	+6	218	+22	$\sim 5$	g',r'	YES
M31 comparison 1	22:27	+31	90	-21	1.2	V,i	PERHAPS
M31-N	0:47	+43:22	123	-19	6.5	V,i	$S/N > 30$
Mono-N	6:03	+64:43	149	+20	1.2	g,r	$S/N > 20$
S223+20 <sup>a</sup>	8:00	+0:00	221	+15	$\sim 10$	g',r'	YES
HVC <sup>b</sup>	17:13	-64:38	327	-15	0.25	g,r	NO

<sup>a</sup> SDSS field, Newberg et al. (2002)

<sup>b</sup> Based on AAT WFI data, Lewis et al. (2002)